J Appl Electrochem (2013) 43:1175–1183
DOI 10.1007/s10800-013-0603-9

RESEARCH ARTICLE

Hydrogen peroxide sensor based on riboflavin immobilized at the nickel oxide nanoparticle-modified glassy carbon electrode

Mahmoud Roushani · Zeinab Abdi · Ali Daneshfar · Abdollah Salimi

Received: 7 June 2013 / Accepted: 3 August 2013 / Published online: 17 August 2013

Abstract A simple and sensitive electrochemical sensor based on nickel oxide nanoparticles/riboflavin-modified glassy carbon (NiONPs/RF/GC) electrode was constructed and utilized to determine H_2O_2. By immersing the NiONPs/GC-modified electrode into riboflavin (RF) solution for a short period of time (5–300 s), a thin film of the proposed molecule was immobilized onto the electrode surface. The modified electrode showed stable and a well-defined redox couples at a wide pH range (2–10), with surface-confined characteristics. Experimental results revealed that RF was adsorbed on the surface of NiONPs, and in comparison with usual methods for the immobilization of RF, such as electropolymerization, the electrochemical reversibility and stability of this modified electrode has been improved. The surface coverage and heterogeneous electron transfer rate constants (k_s) of RF immobilized on a NiO_x–GC electrode were approximately 4.83×10^{-11} mol cm^{-2}, 54 s^{-1}, respectively. The sensor exhibits a powerful electrocatalytic activity for the reduction of H_2O_2. The detection limit, sensitivity and catalytic rate constant (k_{cat}) of the modified electrode toward H_2O_2 were 85 nM, 24 nA μM^{-1} and 7.3 ($\pm$0.2) $\times 10^3$ M^{-1} s^{-1}, respectively, at linear concentration rang up to 3.0 mM. The reproducibility of the sensor was investigated in 10 μM H_2O_2 by amperometry, the value obtained being 2.5 % ($n = 10$). Furthermore, the fabricated H_2O_2 chemical sensor exhibited an excellent stability, remarkable catalytic activity and reproducibility.

Keyword Nickel oxide nanoparticles · Amperometry · H_2O_2 · Riboflavin · Electrocatalytic

M. Roushani (✉) · Z. Abdi · A. Daneshfar
Department of Chemistry, Ilam University, Ilam, Iran
e-mail: mahmoudroushani@yahoo.com

Z. Abdi
e-mail: zeinabadbi20@yahoo.com

A. Daneshfar
e-mail: daneshfar@yahoo.com

A. Salimi
Department of Chemistry, Kurdistan University, Sanandaj, Iran
e-mail: absalimi@yahoo.com

1 Introduction

Hydrogen peroxide (H_2O_2) is a reactive oxygen metabolic by-product that serves as a key regulator for a number of oxidative stress-related states. H_2O_2 is involved in several biological events and intracellular pathways, which have been linked to several diseases [1]. Therefore, its analytical determination becomes of great significance [2].

In comparison with the conventional techniques for H_2O_2 determination, electrochemical technique has been widely used for the detection of hydrogen peroxide because it has inherent advantages of simplicity, easy miniaturization, high sensitivity and relatively low cost [3–7]. In recent years, an increasing effort has been devoted to the development of efficient electrochemical biosensors due to the significance in biological systems and practical applications [8, 9].

Therefore, the development of H_2O_2 sensors with low detection limit and wide concentration range is strongly desired. Due to the slow electrode kinetics and high overpotential required for redox reactions of H_2O_2, the electroanalytical detection of H_2O_2 at bare electrodes is not suited. Electron transfer mediators have been widely used for increasing the electron transfer kinetics and decreasing the required overpotential.

On the other hand, metal oxide particles or nanoparticles are suitable matrices and novel candidates for the immobilization of different redox molecules and biomolecules due to their high electrical conductivity, high surface area, wide electrochemical working window, excellent substrate adhesion, and stable chemical, electrochemical and physical properties. The electrocatalytic activity of different electron transfer mediators, when immobilized onto metal oxide films, is a new challenge in sensor fabrication and electrode modification technologies [10, 11].

From among these, nickel oxide (NiO) nanoparticles have received considerable attention in recent years due to their catalytic, optical, electronic and magnetic properties [12, 13]. Because of the volume, quantum size, surface and macroscopic quantum tunnel effects, nanocrystalline NiO is expected to possess even better properties than those of micrometer-sized NiO particles [14–17]. Based on the unique properties of NiO nanoparticles, they can be used for the immobilization of different molecules. Easy preparation, electroinactivity in physiological pH solutions and high porosity are the advantages of NiO nanomaterials for the entrapment of electron transfer mediators. We have recently reported that NiONPs used for the detection of glycine, L-serine and L-alanine [18].

Riboflavin (6,7-dimethyl9-(d-1-ribityl)-isoalloxazine), commonly called vitamin B_2, is a water-soluble vitamin. Riboflavin is an essential precursor of these coenzymes. The electrochemical behavior of flavins has been studied by several investigations [19–21]. These compounds show reversible two-electron reduction and oxidation waves, both of which are due to overlapping one-electron waves.

In the present study, NiO nanostructures were used for the immobilization of RF. The prepared nanocomposite has been used as an excellent catalyst for H_2O_2 reduction at lower overpotentials. Cyclic voltammetry and amperometry have been used for the investigation of the electrochemical properties and electrocatalytic activity of the nanocomposite-modified electrode. The fabricated sensor was used for the detection of nanomolar concentrations of H_2O_2 and linear concentration range at physiological pH, using hydrodynamic amperometry. To the best our knowledge, up to now, there is no report on the application of NiONPs/RF-modified GC electrode to the detection of H_2O_2.

2 Experimental

2.1 Reagents and solutions

Riboflavin, $Ni(NO_3)_26H_2O$, KCl, $K_4[Fe(CN)_6]$ and other reagents were purchased from Merck and used without purification. H_2O_2 (30 %, w/w) was obtained from Merck, and its diluted solution was prepared daily. The buffer solutions (0.1 M) were made from Na_3PO_4, NaH_2PO_4 and Na_2HPO_4, and the pH was adjusted with 0.1 M H_3PO_4 or 1.0 M NaOH. The pH was measured with a Metrohm model 780 pH/mV meters. Solutions were deaerated by bubbling high-purity (99.99 %) N_2 gas through them prior to the experiments. All electrochemical experiments were carried out at a temperature of 25 ± 0.1 °C.

2.2 Apparatus

All the electrochemical experiments were performed on a μ-AUTOLAB type III and FRA2 board computer-controlled potentiostat/galvanostat (Eco-Chemie, The Switzerland) driven with NOVA software. A conventional three-electrode cell was used with an Ag/AgCl/(sat. KCl) reference electrode, a Pt wire as the counter electrode and a glassy carbon disk (modified and unmodified) as the working electrode. Voltammetry on electrodes coated with NiONPs and RF-modified electrodes was carried out in buffers free of RF molecules. The scanning electron micrographs (SEM) of the electrode surface were obtained by scanning electron microscopy (Philips Company, The Netherlands) at an acceleration voltage of 20 kV. Furthermore, the atomic force microscopy (AFM) (model nanosurf Mobile S software version 1.8) at operating mode of dynamic force and non-contact scan type was used.

2.3 Modification of GC and GC/NiONPs electrodes with RF

Prior to modification, the bare GC electrode (2 mm in diameter) was polished successively with alumina on a polishing cloth and then rinsed with doubly distilled water. The electrodeposition of metallic nickel was carried out using cyclic potential (20 scans between 0 and −1.0 V at a scan rate of 50 mV s^{-1}) in acetate buffer solution, pH 4, a solution containing 1 mM nickel nitrate. The potential was repetitively cycled (30 scans) from 0 to 1.0 V at a scan rate of 100 mV s^{-1} in fresh phosphate solution for the electrodissolution and passivation of a nickel oxide layer at a GC electrode [22]. Simple adsorption method was used for immobilization of RF onto nickel oxide nanostructures.

After the electrodeposition of nickel oxyhydroxide nanomaterials onto GC electrode, the NiO/GC electrode cycling the potential 0.0 V and 1.6 V (30 cycles) at a scan rate of 100 mV s^{-1}, in pH 7 phosphate buffer solutions (0.1 M) and then the electrode was immersed in fresh phosphate solution containing 0.1 mM RF for 5–300 s. A stable thin film of the RF was adsorbed on the electrode surfaces. The electrode surface is rinsed with deionized water before using. The same procedure was used for bare GC electrode in the presence of RF. The effective surface area of the

electrode modified with NiONPs was determined to be 0.11 cm^2 from the cyclic voltammogram of 1 mM $K_3[Fe(CN)_6]$ in buffer solution, pH 7.

3 Results and discussion

3.1 Electrochemical properties of modified electrode

The formation and growth of electrodeposited NiONPs on a GC electrode were investigated by SEM and AFM (Fig. 1a, b). As shown, nickel oxide particles grow by electrodeposition on the amorphous GC electrode surface. The average size of the NiO particle varies from under 50 nm to slightly less than 200 nm. AFM images also show nickel oxide nanostructures with average diameters ranging from 50 to 200 nm electrodeposited on the GC electrode. Furthermore, the electrodeposition of the nickel oxide layer on the electrode surface was verified by recording cyclic voltammograms of the modified electrode in alkaline solution (not shown). The cyclic voltammogram exhibits an anodic peak at 0.4 V and a cathodic peak at 0.35 V, due to the oxidation of the $Ni(OH)_2$ phase to NiO(OH) and the reduction of $NiO_x(OH)$ to $Ni(OH)_2$ [23].

The electrochemical impedance spectroscopy is an efficient tool to probe the features of surface-modified electrode. The electron transfer resistance of the electrochemical reaction, R_{et}, corresponds to the semicircle diameter of the Nyquist plot of $-Z''$ against Z' and it reveals the electron transfer kinetics of the redox electrochemical probe at the electrode interface. Figure 2 shows impedance spectra on a bare GC electrode (a) and a NiONPs/GC (b) electrode, respectively. It can be seen that the R_{et} of the NiONPs/GC electrode (curve b) significantly decreases compared to the GC electrode (curve a), attributing to the excellent conductivity of NiONPs.

Figure 3 shows the cyclic voltammograms of NiO, NiO/RF-modified GC electrodes in buffer solution (pH 7). As shown for the NiO_x-modified GC electrode, no redox peaks were observed (voltammogram "a") at a potential range of 0.2 to −0.7 V, which provides a potential window of the NiO/GC electrode for investigating the voltammetric behavior of RF. By immersing the GC/NiO-modified electrode in 0.1 mM RF solution for 300 s, a stable thin layer of RF was adsorbed. As shown for GC electrodes modified with NiONPs and RF, a well-defined cyclic voltammogram with a peak potential separation of less than 30 mV and a peak current of 0.4 μA was observed at a formal potential of 0.41 V (Fig. 3 voltammogram "b"). This result indicates that the porous interfacial layer of the nano-NiO-modified electrode with a high specific surface area increases the conductive area and RF can penetrate through the conductive porous channels onto the electrode more easily, leading to a higher redox response, and the reversibility of RF is significantly improved.

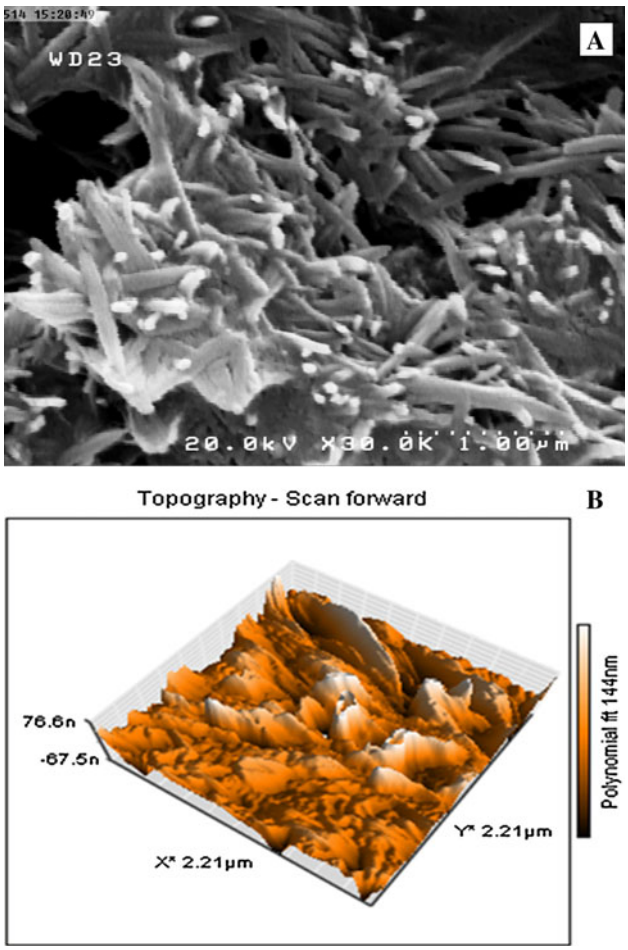

Fig. 1 **a** SEM image of the electrodeposited nickel oxide on glassy carbon, *scale bar* is 1 μm. **b** AFM images of the electrodeposited NiONPs sample

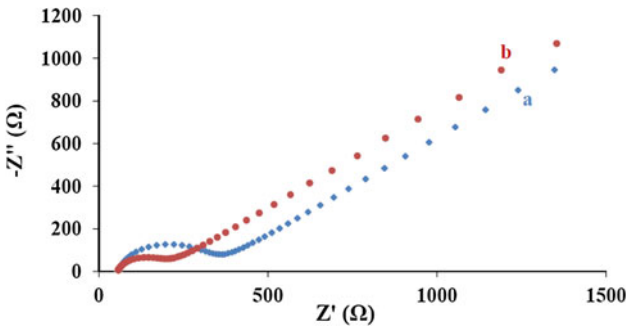

Fig. 2 Electrochemical impedance spectra of **a** bare GC, and **b** NiONPs/GC electrode

The electrochemical properties of GC/NiO nanoparticles modified with RF were compared with those of GC electrode modified with the proposed RF using physical adsorption as the modification technique. As shown in inset

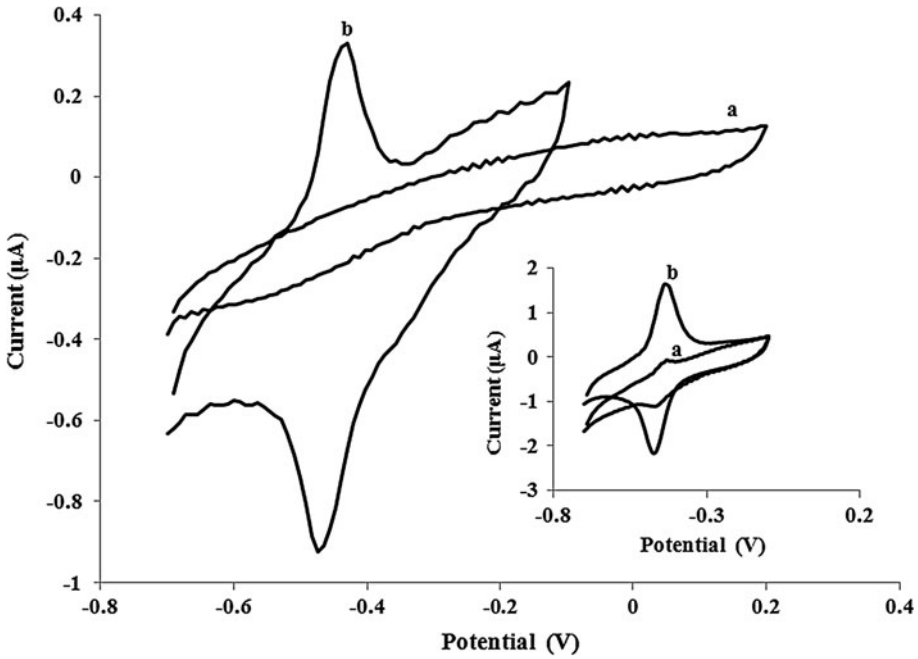

Fig. 3 Cyclic voltammograms of: **a** GC electrode, modified with NiONPs in 0.1 M phosphate buffer solution (pH 7), **b** GC electrode, modified with NiONPs and RF under the conditions presented in (*a*), with an immersion time for electrode modification of 300 s, and a scan rate of 20 mV s^{-1}. The inset shows the cyclic voltammograms of: *a* GC electrode, modified with RF. *b* GC electrode, modified with NiONPs and RF in 0.1 M phosphate buffer solution (pH 7) and a scan rate of 100 mV s^{-1}

of Fig. 3a, by immersing the preanodized GC electrode in 0.1 mM RF solution for 20 min, a cyclic voltammogram with low peak current (0.04 μA) was observed.

Figure 4a demonstrates the cyclic voltammograms of a GC electrode modified with the RF/NiO film in buffer solution pH 7, at different scan rates. Figure 4b explains the plots of the anodic and cathodic peak currents versus the scan rate for the modified electrode. Both the anodic and cathodic peak currents are linearly proportional to the scan rate in the range of 10–6,000 mV s^{-1}, indicating a surface-confined electrode process. Moreover, redox potentials are almost the same at the different scan rates, indicating that RF adsorbed onto the surface undergoes a reversible electron transfer with the NiONPs. The peak-to-peak separation is about 20 mV at scan rates below 100 mV s^{-1}, suggesting facile charge transfer kinetics over this range of sweep rates.

According to the slope of the I_p versus v curve and the following equation, the surface concentration (Γ_c) of RF on the surface of NiONPs-modified GC electrode was estimated [24].

$$I_p = \frac{n^2F^2vA\Gamma_c}{4RT}, \quad (1)$$

where v is the sweep rate, A is the effective surface area (0.11 cm^2) of the modified electrode, and the other symbols have their usual meaning. From the slope of cathodic peak currents versus scan rate, the calculated surface concentration of RF is 4.83×10^{-11} mol cm^{-2}. At higher sweep rates, the plot of peak currents versus scan rate deviates from linearity and the peak current becomes proportional to the square root of the scan rate (Fig. 4c), indicating a diffusion-controlled process. The slow diffusion of counter ions (H^+) into the electrode surfaces controlled the electrochemical reaction. At higher sweep rates ($v >$ 5,000 mV s^{-1}), peak separations begin to increase, indicating the limitation due to charge transfer kinetics.

Based on Laviron's theory [25], the electron transfer rate constant (k_s) and charge transfer coefficient (α) can be determined by measuring the variation of peak potential with scan rate. The values of peak potentials were proportional to the logarithm of the scan rate for scan rates higher than 5 V s^{-1} (Fig. 4d). The slope of the ΔE_c versus log (v) was about 64 mV ($\Delta E_c = E_{pc} - E^0$). Using the equation $E_p = K - 2.3030(RT/\alpha nF)$ log v and the two electrons transferred for RF, a charge transfer coefficient, $\alpha = 0.46$, was obtained. Introducing this α value in the following equation [25],

$$\log k_s = \alpha \log(1-\alpha) + (1-\alpha)\log\alpha - \log\left(\frac{RT}{nFv}\right) - \alpha(1-\alpha)\left(\frac{nF\Delta E}{2.3RT}\right), \quad (2)$$

an apparent surface electron transfer rate constant, $k_s = 54 \pm 0.1$ s^{-1}, was estimated.

The large value of the electron transfer rate constant indicates a high ability of NiONPs for promoting electrons between RF and the electrode surface.

3.2 Stability, reproducibility and pH dependence of the RF/NiO-modified electrode

The stability of the NiO/RF-modified GC electrode was examined by continuous potential cycling between −0.1

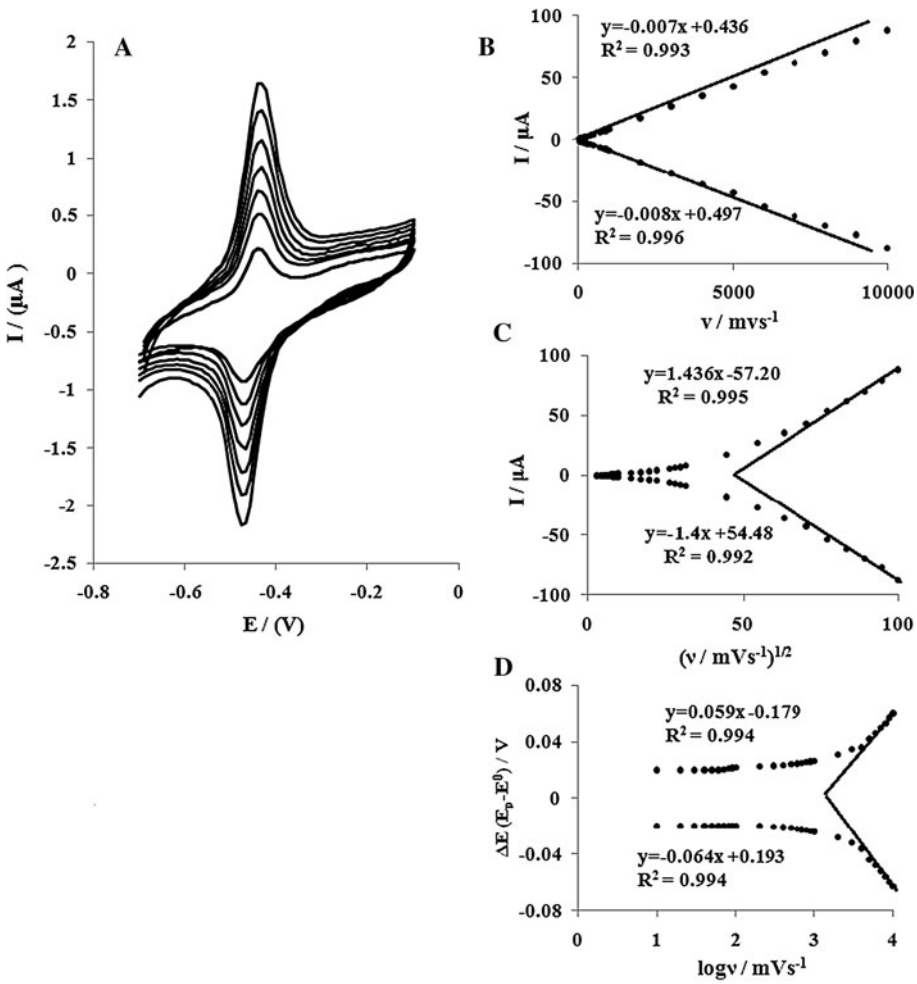

Fig. 4 **a** Cyclic voltammetric responses of a NiO/RF-modified GC electrode in phosphate buffer (pH 7) at scan rates (inner to outer) of 30, 40, 50, 60, 70, 80 and 90 mV s^{-1}. **b**, **c** Plots of peak currents versus the scan rate and square root of scan rate. **d** Variation in peak potential versus log *v*

and −0.7 V in 0.1 M phosphate buffer solution (pH 7; not shown). The results indicated that after 100 repetitive cycles at a scan rate of 150 mV s^{-1}, no detectable change was observed at the peak height and potential separation. In addition, it was found that the current value is decreased only by 7 % when the electrode was immersed in buffer solution (pH 7) for 24 h.

The stability of the modified electrodes was evaluated by the same method in electrolyte solutions at pH 2 and 10. The results indicated that the modified electrode was stable in acidic and alkaline solution. Since the method of electrode preparation is simple and fast (less than 10 min), the current decay is not a serious disadvantage for this modified electrode. The high stability of adsorbed RF against desorption in aqueous solution is related to the chemical and mechanical stability of the NiO film and the strong adsorption of RF on the surface of NiONPs.

The reproducibility of the sensor was evaluated by amperometry. The relative standard deviation (RSD) for 10 repeated measurements (in 10 μM H_2O_2) with the same NiO/RF-modified GC electrode was 2.5 %. For 5 NiO/RF-modified GC electrodes, the RSD was 3.6 %. These results indicate that the proposed sensor has excellent reproducibility.

For investigating the effect of pH on the redox response of modified electrodes, cyclic voltammograms of the NiO/RF-modified GC electrode at various pH values were recorded. Figure 5 explains that the film exhibited a single redox couple in the pH range $2 < pH < 10$. The electrochemical behavior of NiO/RF-modified GC electrode was studied at different pH using cyclic voltammetry. Anodic and cathodic peak potentials of the NiO/RF-modified GC electrode were shifted to less positive values with increasing of pH. A potential pH diagram, plot of the $E^{0'}$ as a function of pH, is composed of a straight line with a slope of 59 mV pH^{-1}. Therefore, the electro-oxidation of RF obeys the Nernst equation for a two-electron and two-proton transfer reaction [26].

3.3 Electrocatalytic activity of NiO/RF-modified GC electrode for reduction of H_2O_2

Due to chemical stability, electrochemical reversibility and high electron transfer rate constant of RF at the NiONPs-

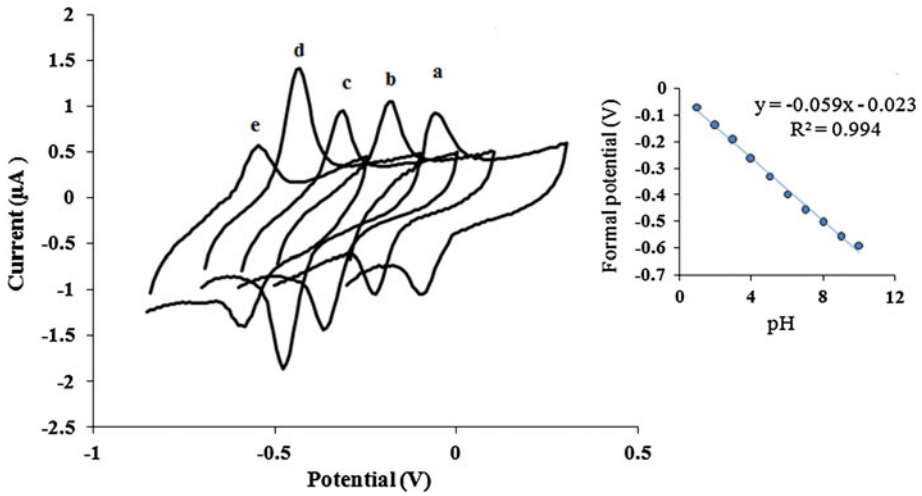

Fig. 5 Cyclic voltammetric response of a NiO/RF-modified GC electrode at different pH 2, 4, 6, 8 and 10 (from *right* to *left*); scan rate 50 mV s^{-1}. *Inset* shows the variation in standard potentials versus pH values

modified GC electrode, it can be used as a mediator to shuttle electron between electrodes and analyte molecules. In order to test the potential electrocatalytic activity of the NiO/RF-modified GC electrode, its cyclic voltammetric responses at 25.0 mV s^{-1} were obtained in buffer solution (pH 7.0) in the presence of 0.08 mM RF and the data are presented in Fig. 6. Curves (a) and (c) show cyclic voltammograms of NiONPs-modified GC electrode and NiO/RF-modified GC electrode, respectively, in buffer solution without H_2O_2. Curves (b) and (d) show the reduction peak of NiONPs-modified GC electrode and NiO/RF-modified GC electrode in the presence of H_2O_2. For NiO-modified GC electrode, no redox response for H_2O_2 reduction can be seen in the potential range from 0.20 to −0.8 V (voltammogram "b"). The decrease in overvoltage and increase in the peak current of H_2O_2 reduction confirm that RF has high catalytic ability for H_2O_2 reduction. Therefore, RF immobilized onto NiONPs is suitable as mediators to shuttle electron between H_2O_2 and working electrode and facilitate electrochemical regeneration following electron exchange with H_2O_2.

Cyclic voltammograms of the modified electrode in the presence of different concentrations of H_2O_2 were recorded (Fig. 7). Inset of Fig. 7 shows the plot of catalytic current (at potential −0.32 V) versus H_2O_2 concentration. As shown, peak current linearly increased with an increase in the concentration of H_2O_2 and the calibration plot is linear (correlation coefficient, 0.998) for low concentrations (20–100 μM). The sensitivity and the detection limit (3σ) of the sensor toward H_2O_2 were found to be 0.016 μA μM^{-1} and 1.0 μM, respectively.

The cyclic voltammograms of modified electrode in buffer solution containing H_2O_2 at different scan rates were recorded (Fig. 8a). The peak current for the reduction of H_2O_2 is proportional to the square root of the scan rate, suggesting that the process is controlled by diffusion as expected for a catalytic system. It can also be noted that by

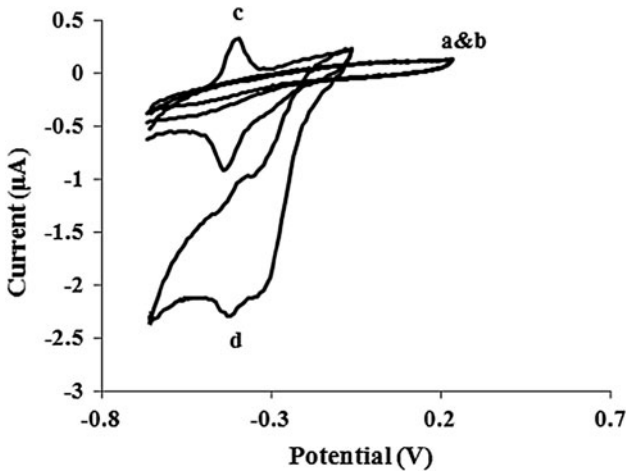

Fig. 6 Recorded cyclic voltammograms of a GC electrode, modified with NiONPs in phosphate buffer solution (pH 7) at scan rate 25 mV s^{-1} **a**; **b** as **a** in the presence of 0.08 mM H_2O_2; **c** and **d** as **a** and **b** for GC electrode, modified with NiONPs and RF

increasing the sweep rate, the peak potential for the catalytic reduction of H_2O_2 shifts to more negative values, suggesting a kinetic limitation in the reaction between the redox sites of RF and H_2O_2. Also, a plot of the scan rate-normalized current ($I_p/v^{1/2}$) versus scan rate (Fig. 8b) exhibited the characteristic shape of a typical *EC′* catalytic process [27]. Based on the obtained results, the following catalytic scheme describes the reaction sequence in the reduction of oxidation of H_2O_2 with RF.

$$\text{Riboflavin (oxdidized form)} + 2H^+ + 2e^- \rightarrow \text{riboflavin(reduced form)} \quad (3)$$

$$\text{Riboflavin (reduced form)} + H_2O_2 \xrightarrow{K_{cat}} \text{riboflavin (oxdidized form)} + 2H_2O \quad (4)$$

For an *EC′* mechanism, the Andriex and Saveant theoretical model [28] can be used to calculate the catalytic rate

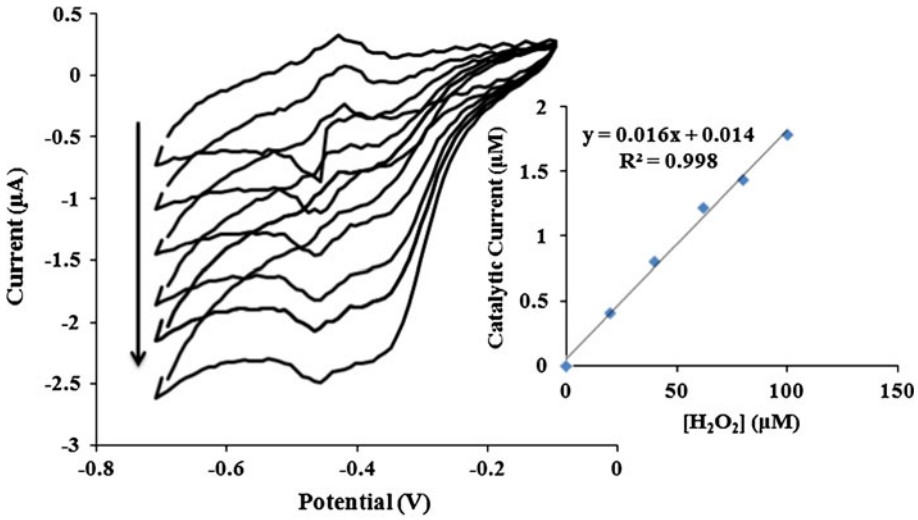

Fig. 7 Cyclic voltammograms of GC electrode, modified with NiONPs and RF in the presence of different concentrations of H_2O_2 in buffer solution ((pH 7) from inner to outer 0, 20, 40, 60, 80 and 100 μM. at scan rate of 20 mV s^{-1}. The *inset* shows the catalytic response versus H_2O_2 concentrations

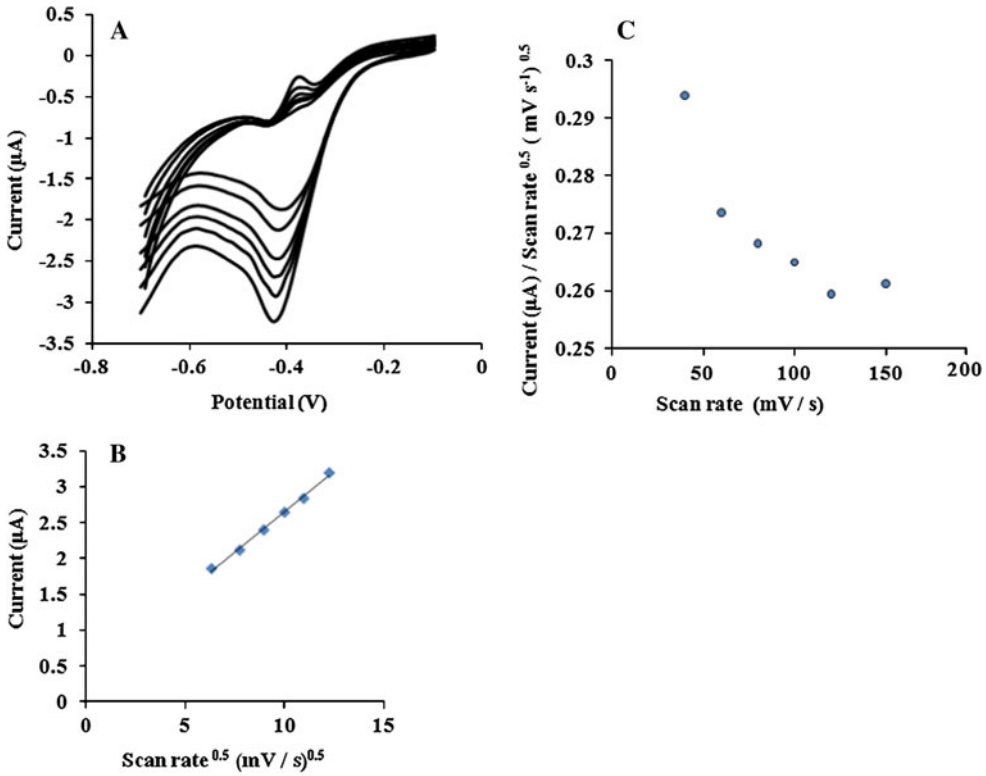

Fig. 8 **a** Cyclic voltammetry response modified GC electrode in pH 7 at buffer solution containing 0.08 mM of H_2O_2 at different scan rates of (from *inner* to *outer*) 40, 60, 80, 100, 120, and 150 mV s^{-1}. **b** Plot of peak current versus $v^{1/2}$. **c** Plot of $I_p/v^{1/2}$ versus v

constant. Based on this theory, a relation between the peak current and the concentration of substrate for slow scan rates and large catalytic rate constant exists:

$$I_p = 0.44nFAD^{1/2}\left(\frac{vF}{RT}\right)^{\frac{1}{2}}C_s, \quad (5)$$

where D and C_s are the diffusion coefficient (cm^2 s^{-1}) and the bulk concentration (mol cm^{-3}) of substrate (hydrogen peroxide), respectively, and other symbols have their usual meanings. Low values of K_{cat} result in values of the coefficient lower than 0.496. For low scan rates (5–20 mV s^{-1}), the average value of this coefficient was found to be 0.30 and 0.33 for a NiONPs/RF-modified GC electrodes, with a coverage of 4.83×10^{-11} mol cm^{-2} and a geometric area (A) of 0.11 cm^2 in 0.1 mM hydrogen peroxide at pH 7. According to the approach of Andriex and Saveant, and using Fig. 1 in Ref. [28], the average values of the calculated K_{cat} are 7.3 (± 0.2) $\times 10^3$ M^{-1} s^{-1} for modified electrode.

3.4 Amperometric detection of H_2O_2 at NiO/RF-modified GC electrode

Since amperometry under stirred conditions has a much higher current sensitivity than cyclic voltammetry, it was

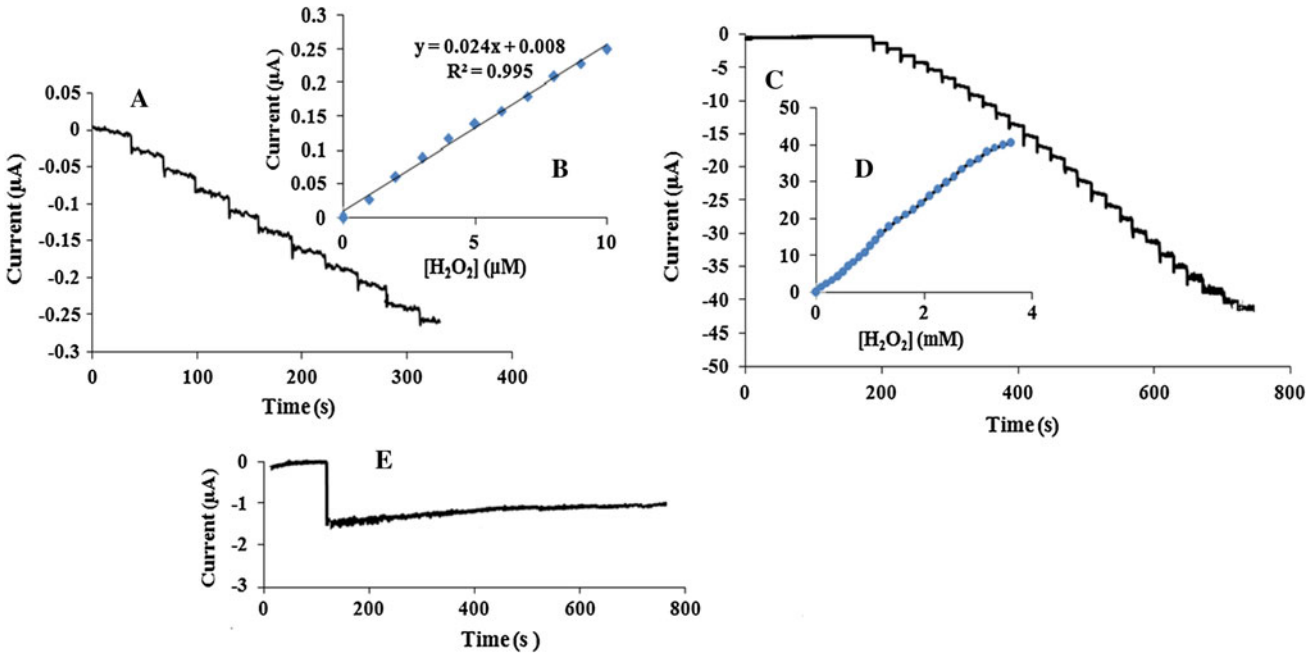

Fig. 9 Amperometric response for a rotating modified NiONPs/RF GC electrode at rotation speed 1,000 rpm and −0.32 V in a pH 7 solution for successive additions of **a** 1 μM and **c** 0.10 mM H_2O_2. **b** and **d** Plots of chronoamperometric currents versus H_2O_2 concentrations. **e** Recorded chronoamperogram for 60 μM H_2O_2 during 10 min

used to estimate the lower limit of detection for the proposed electrochemical system. As discussed above, the proposed modified electrode showed excellent and strong mediation properties to facilitate the low potential amperometric measurements of hydrogen peroxide. Figure 9a shows a typical current–time plot of the rotated modified GC electrode (rotation speed 1,000 rpm) on successive additions of 1.0 μM of hydrogen peroxide at an applied potential of −0.32 V (vs. Ag/AgCl). As shown, the modified electrode responded rapidly and approached 95 % of the steady-state current within 3 s.

The plot of current response versus H_2O_2 concentration is shown in the Fig. 9b. The calibration plot is linear over a wide concentration range (1 μM–4 mM), while for a high concentration of H_2O_2, the plot of current versus analyte concentration deviates from linearity (Fig. 9d). The linear least squares calibration curve over the range of 1–10 μM (ten points) is I (μA) = 0.024 [H_2O_2] μM + 0.008 μA with a correlation coefficient of 0.995, indicating that the regression line is fitted very well with the experimental data and the regression equation can be applied in the unknown sample determination. The detection limit (when signal to noise ratio was 3) and sensitivity were 85 nM and 24 nA μM^{-1}, respectively. Highly stable amperometric response toward hydrogen peroxide is extremely attractive feature of the NiO/RF-modified GC electrode. Figure 9e shows the amperometric response of 60 μM H_2O_2 during a prolonged 700-s experiment. The response remains stable throughout the experiment (only a 4 % decrease in current was observed), indicating that riboflavin is effectively stabilized with immobilization onto nickel oxide nanomaterials. Therefore, the modified electrode possesses excellent, stable and strong mediation properties and facilitates the low potential amperometric measurement of H_2O_2 at trace levels.

4 Conclusions

The present study shows that GC electrode, modified with NiONPs/RF, can be used as sensitive amperometric hydrogen peroxide sensors. The immobilized RF shows good stability and electrochemical reversibility at wide pH range due to their excellent biocompatibility of nickel oxide nanostructures. Cyclic voltammetric results indicate that electrocatalytic reduction of H_2O_2 at NiO/RF-modified GC electrode exhibits the characteristic shape typical of an *EC′* mechanism. The resulting biosensor exhibits many advantages, such as high sensitivity, low detection limit, wide concentration range, good reproducibility and storage stability. Detection limit, response time sensitivity and linear concentration range of NiO/RF-modified GC electrode were 85 nM, 3 s, 24 nA μM^{-1} and 1 μM–3.5 mM, respectively. These analytical parameters are comparable or better than the results reported for H_2O_2 determination at the surface of other modified electrodes. Owing to high biocompatibility, high adsorption ability and little harm to the biological activity of nickel oxide nanomaterials, the composition of

these nanostructures and biomolecules may be favorable for construction of biosensors and bioelectronic devices.

References

1. Yan Q, Wang Z, Zhang J, Peng H, Chen X, Hou H, Liu C (2012) Electrochim Acta 61:148–153
2. Ye DX, Xu YH, Luo LQ, Ding YP, Wang YL, Liu XJ, Xing LJ, Peng JW (2012) Colloids Surf B 89:10–14
3. Chen W, Cai S, Ren QQ, Wen W, Zhao YD (2012) Analyst 137:49–58
4. Noorbakhsh A, Salimi A (2009) Electrochim Acta 54:6312–6321
5. Noorbakhsh A, Salimi A, Sharifi E (2008) Electroanalysis 20:1788–1797
6. Salimi A, Noorbaksh A, Soltanian S (2006) Electroanalysis 18:703–711
7. Salimi A, Rahmatpanah R, Hallaj R, Roushani M (2013) Electrochim Acta 95:60–70
8. Krishnamoorthy K, Gokhale RS, Contractor AQ, Kumar A (2004) Chem Commun 7:820–821
9. Kros A, Van Hovell SWFM, Sommerdijk NAJM, Nolte RJM (2001) Adv Mater 13:1555–1557
10. Yavuzn Y, Koparal AS (2006) J Hazard Mater 136:296–302
11. Manea F, Radovan C, Schoonman J (2006) J Appl Electrochem 36:1075–1081
12. Carnes CL, Klabunde KJ (2003) J Mol Catal A 194:227–236
13. Ichiyanagi Y, Wakabayashi N, Yamazaki J, Yamada S, Kimishima Y, Komatsu E, Tajima H (2003) Phys B 862:329–333
14. Wu L, Wu Y, Wei H, Shi Y, Hu C (2004) Mater Lett 58: 2700–2703
15. Yi X, Zhong D (2004) Mater Lett 58:276–280
16. Tao DL, Wei F (2004) Mater Lett 58:3226–3228
17. Biju V, Khadar MA (2003) Spectrochim Acta, Part A 59:121–136
18. Roushani M, Shamsipur M, Pourmortazavi SM (2012) J Appl Electrochem 42:1005–1011
19. Breyer B, Biegler T (1960) Collect Czec Chem Commun 25:3348–3360
20. Hartley AM, Wilson GS (1966) Anal Chem 38:681–687
21. Gorton L, Johansson G (1980) J Electroanal Chem 113:151–158
22. Kong XY, Ding Y, Yang R, Wang ZL (2004) Science 303: 1348–1351
23. Giovanelli D, Lawrence NC, Jiang L, Jones TGL, Compton RG (2003) Sens Actuators, B 88:320–328
24. Brown AP, Anson FC (1997) Anal Chem 49:1589–1595
25. Lavion E (1979) J Electroanal Chem 101:19–28
26. Qijin W, Nianjun Y, Haili Z, Xinpin Z, Bin X (2001) Talanta 55:459–467
27. Pariente E, Lorenzo E, Tobalina F, Abruna HD (1995) Anal Chem 67:3936–3944
28. Andriex CP, Saveant JM (1978) J Electroanal Chem 93:163–168